Impact of divertor material on neutral recycling and discharge fueling in DIII-D

I Bykov[1,6] , **D L Rudakov**[1] , **A Yu Pigarov**[1], **E M Hollmann**[1], **J Guterl**[2] ,
J A Boedo[1] , **C P Chrobak**[3] , **T Abrams**[3] , **H Y Guo**[3], **C J Lasnier**[4],
A G McLean[4], **H Q Wang**[3], **J G Watkins**[5] and **D M Thomas**[3]

[1] University of California San Diego, La Jolla, CA 92093-0417, United States of America
[2] Oak Ridge Associated Universities, Oak Ridge, TN 37831-0117, United States of America
[3] General Atomics, San Diego, CA 92186-5608, United States of America
[4] Lawrence Livermore National Laboratory Livermore, CA 94550, United States of America
[5] Sandia National Laboratory, Livermore, CA 94551-0969, United States of America

E-mail: ibykov@ucsd.edu

Abstract

Experiments with the lower divertor of DIII-D during the Metal Rings Campaign (MRC) show that the fraction F of atomic D in the total recycling flux is material-dependent and varies through the ELM cycle, which may affect divertor fueling. Between ELMs, $F_C \sim 10\%$ and $F_W \sim 40\%$, consistent with expectations if all atomic recycling is due to reflections. During ELMs, F_C increases to 50% and F_W to 60%. In contrast, the total D recycling coefficient including atoms and molecules R stays close to unity near the strike point where the surface is saturated with D. During ELMs, R can deviate from unity, increasing during high energy ELM-ion deposition (net D release) and decreasing at the end of the ELM which leads to ability of the target to trap the ELM-deposited D. The increase of $R > 1$ in response to an increase in ion impact energy E_i has been studied with small divertor target samples using Divertor Materials Evaluation System (DiMES). An electrostatic bias was applied to DiMES to change E_i by 90 eV. On all studied materials including C, Mo, uncoated and W-coated TZM (>99% Mo, Ti, and Zr alloy), W, and W fuzz, an increase of E_i transiently increased the D yield (and R) by $\sim$10%. On C there was also an increase in the molecular D_2 yield, probably due to ion-induced D_2 desorption. Despite the measured increase in F on W compared to C, attached H-mode shots with OSP on W during MRC did not demonstrate a higher pedestal density. About 8% increase in the edge density could be seen only in attached L-mode scenarios. The difference can be explained by higher D trapping in the divertor and lower divertor fueling efficiency in H- versus L-mode.

Keywords: DIII-D, tokamak, tungsten, recycling, fueling

(Some figures may appear in colour only in the online journal)

1. Introduction

The quest for materials suitable for plasma facing components (PFCs) of magnetic confinement fusion devices is driven by stringent requirements to their thermo-mechanical, chemical, and radiation properties: melting point, ductility, thermal diffusivity, physical and chemical erosion rates and maximum permissible concentration in the plasma, H diffusivity, ability

to form bonds and co-deposit with H, and effects of high dose neutron irradiation. Still widely used for PFCs, graphite has a number of advantages including high thermal diffusivity, no melting, relatively low charge number $Z_C = 6$, which provides very forgiving operation of tokamaks with a graphite first wall. Nevertheless, because of high co-deposition rates with H and its radiation-induced embrittlement graphite has largely been discarded as a PFC material for burning plasma applications. The next generation tokamak ITER as well as the largest present-day machine JET with ITER-Like Wall

[6] Author to whom any correspondence should be addressed.

(JET-ILW [1]) have a similar combination of PFC materials: Be in the main chamber and W in the divertor. Several other machines including ASDEX-Upgrade (AUG [2]) have transitioned from full-C to fractional W divertor and wall coverage. Recycling on PFC surfaces constitutes a strong intrinsic source of neutral deuterium for plasma fueling. Therefore, a change to the PFC composition may be expected to affect the energy and the flux of the neutral D through the change of the particle and energy reflection coefficients.

It has been noted upon transition to JET-ILW that some properties of the H-mode pedestal and plasma performance have changed compared to JET-C due to the difference in the PFC materials. The pedestal degradation and the decrease of the ELM stability are associated with a larger relative shift between the pedestal n_e and T_e profiles and smaller normalized pressure gradient in JET-ILW [3]. The effect of the material change was similar to an increase of the gas puff rate in JET-C [3]. A lower L-H transition power threshold seen in both JET-ILW and AUG was also associated with the materials change [4]. In contrast to JET-ILW and AUG, in DIII-D only a small fraction (0.6%) of the total wall area was replaced with W-covered inserts in a dedicated metal rings campaign (MRC) in 2016. In this work we study the consequences of the material change in the divertor of DIII-D for the local neutral fuel sourcing and the edge profile modification.

2. Experimental approach

DIII-D is a full-C tokamak with major and minor radii of 1.67 m and 0.67 m, respectively [5]. DIII-D has a versatile suite of edge and divertor diagnostics that are described in [6–8], including CO_2 interferometers, core and edge Thomson scattering (TS), charge exchange recombination spectroscopy (CER), filtered photomultipliers (filterscopes), and filtered cameras, including IR cameras for surface temperature and heat flux measurements. The shelf of the lower outer divertor is equipped with the Divertor Material Evaluation System (DiMES) [7], allowing exposure of material samples aligned with the divertor surface. DiMES can be used to study local recycling on multiple circular 6 mm diameter samples made of different materials. An example of the DiMES head design is given in [8]. DiMES samples can be electrically biased to change the ion incidence energy E_i. In L-mode discharges biasing DiMES allowed the study of the recycling response to an E_i increase, similar to what happens during an ELM due to the initial high-energy ion component.

Simultaneous time and spatially resolved measurements of atomic (D) and molecular (D_2) deuterium recycling fluxes were made with absolutely calibrated split filtered imaging of the lower divertor using atomic D_α emission (656 nm) and molecular Fulcher-band (600–640 nm) emission. The time and spatial resolutions of these measurements are 2 ms and 3 mm. General aspects of fast imaging on DIII-D are described in [9]. The split imaging was used to calculate the fraction

of the atomic deuterium F in the recycling flux [10]:

$$F = \frac{\Gamma_{Acy}}{\Gamma_{Acy} + 2\Gamma_M} \simeq 1 - \frac{2}{\dfrac{\Phi(D_\alpha)}{\Phi(D_2)} \dfrac{S/XB(D_\alpha)}{D/XB(D_2)} + 1} \quad (1)$$

Γ_A and Γ_M are atomic and molecular deuterium recycling fluxes, Φ is the measured photon flux, S/XB [11] and D/XB [12] are inverse photon efficiencies with respect to D ionization and D_2 dissociation.

Any change in the recycling properties of DiMES samples is local and therefore does not influence the global plasma performance. Such a study of the global impact of a PFC material change would require replacing a fraction of the PFC area with a toroidally symmetric array of components made of a different material. In June–July 2016, the lower divertor of DIII-D has been modified by inserting 2 toroidally continuous 5 cm wide W-coated TZM (an alloy with >99% of Mo) rings. The month-long mini campaign that followed was called the MRC [6]. The main objective of MRC was to study W sourcing and transport in a low-Z environment. Our focus in this work will be on the effect of adding W in the divertor on local recycling and its consequences for fueling and modification of midplane plasma profiles. In order to maintain the purity of the W and avoid its coating with re deposited C in the otherwise full-C machine, majority of the campaign was comprised of scenarios with attached outer strike point (OSP). The satisfactory condition of the Rings was verified by *in situ* monitoring of the WI yield and visible-range camera imaging. Between-shots and post mortem inspection revealed no C build up. Some C was found post mortem in recessed areas of the rough W surfaces.

3. Results and discussion

3.1. Small-scale DiMES material tests

A set of metal samples including C, Mo, uncoated and W-coated TZM (>99% Mo), W, and W fuzz, were exposed on DiMES in a series of L-mode shots with $T_e = 28$ eV at OSP placed on the inboard side of DiMES. The plasma parameters near the target were measured with Langmuir probes (LPs) and constrained with divertor Thomson scattering data. A rectangular bias signal V_b consisting of $+10$ and -80 V phases with respect to the ground was applied to DiMES in order to modulate the ion impact energy. Keeping $V_b \ll V_p$ (the plasma potential), keeps the collected ion current I_b saturated. This helps isolate the effect of the ion energy E_i increase during ELMs from the particle flux increase.

Figure 1 shows the relative change of the total and molecular deuterium flux upon an increase of the ion incidence energy (E_i) due to a change in the applied bias. The plotted quantity is an equivalent of R–1 for the total (atomic and molecular) and molecular deuterium, where R is the recycling coefficient. The time vector is centered at the time when V_b is switched from $+10$ to -80 V, and the data is obtained by coherently averaging over $\sim$10 V_b cycles. E_i increases by

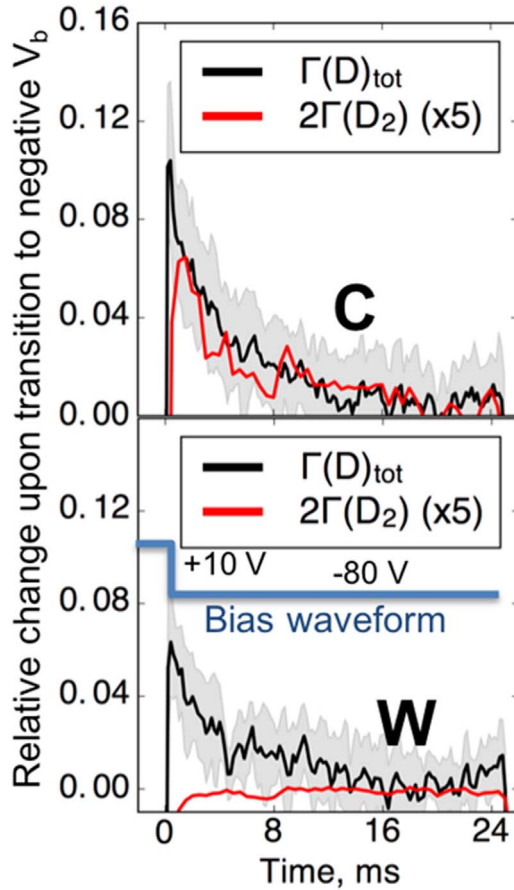**Figure 1.** Relative change of the total $\Gamma(D)_{tot} = \Gamma(D) + 2\Gamma(D_2)$ and molecular $2\Gamma(D_2)$ deuterium recycling fluxes on C and on W on DiMES in response to an E_i increase by 90 eV. The baseline signal is subtracted. Both materials show a similar ~10% increase in the total recycled D.

90 eV from $E_i \simeq 3T_e + 2T_i - 10$ eV ≈ 130 eV $(T_i \approx T_e)$ during the positive bias phase to 220 eV during the negative phase which leads to a transient increase of both the total neutral D flux and its molecular fraction on C. On W there is no increase of the D_2 component, therefore the increase of the total D is only due to atoms. The relative atomic concentration of surface D at saturation decreases with E_i [13]. Therefore, surface becomes super-saturated with D when E_i suddenly increases, and the excess D is promptly released. About 20 ms after V_b changes, the recycling coefficient R stabilizes close to unity due to surface saturation.

The D re-emission peak at $t = 0$ s cannot be explained by an increase of the surface temperature T_{surf}. Measured by a calibrated IR camera T_{surf} increased from $50\,^{\circ}C$ to $350\,^{\circ}C$ during one discharge with $<20\,^{\circ}C$ increments during the negative bias phases. Due to its exponential dependence on $-E_{act}/kT_{surf}$ and the activation energy E_{act} of the order of a few eV, the thermal desorption rate at these temperatures is low and adding $20\,^{\circ}C$ is not expected to lead to a noticeable change.

The peak at $t = 0$ ms is attributed to a depletion of the surface reservoir by more energetic D^+ ions and implies that, temporarily, $R > 1$ because the incident ion flux density is

not changing. A similar effect was probably seen on graphite saturated by D at implantation energy 1 keV when the beam energy was switched to 6 keV [13]. In a tokamak experiment a similar depletion of the surface D reservoir is probably what causes a short D_α spike when the limiter bias is turned on at -200 V, see in [14]. The ion induced de-trapping of molecular D in saturated graphites has been explained and modeled by the recombination of beam-activated and trapped atomic D in the bulk within the implantation depth and its quick diffusion to the surface through micro cracks and pores [15]. This mechanism may be nonexistent in W which explains why there is no D_2 spike in response to an E_i increase on W. The D peak on both W and C is probably due to a direct sputtering of the saturated surface D layer. Other studied metals behaved similar to W.

In ELMy H-modes both E_i and the flux density of D^+ ions increase during ELMs and R will depend on the balance between the deposition of energetic ions and induced desorption of the near-surface D. Regimes with $R \approx 1$ [16] and $R > 1$ [17] in the divertor have been previously discussed. The transiently released D increases the local plasma density, which may lead to a transient higher recycling regime [18] or even detachment after an ELM. On C this can be aided by the higher fraction of molecules in the recycling flux that can contribute to the power and momentum dissipation and can help achieve detachment through molecule assisted recombination [19].

Regimes with $R > 1$ during ELMs are attractive because they lead to a reduction of the wall gas loading. This can be realized in the main chamber when ELM filaments interact with the vessel wall, and would explain the observation made in [20] of a drop in the wall gas loading upon the L-H transition.

The slow desorption of D_2 between ELMs supplies fuel for pedestal recovery. D_2 desorbs at about the wall temperature, and Frank–Condon D atoms due to D_2 dissociation have energy of the order of 2 eV and are ionized in the scrape off layer (SOL) before reaching the separatrix. In order to gain sufficient energy to cross the separatrix, the low-energy deuterium due to desorption has to either undergo a charge-exchange collision with an edge ion or become ionized and reflect from the divertor target. This is why the inter-ELM reflection properties of the divertor material become important. The two material-related quantities responsible for fueling are the energy- and the particle-reflection coefficients. Both are higher on W than on C; therefore, one expects more efficient divertor fueling with W in the divertor.

3.2. Large scale W-divertor experiment during MRC

During MRC, the split imaging of the lower divertor was performed keeping the W Ring within the camera view. The fractions of recycled atoms F_C and F_W were calculated using equation (1) for a low-heated Type-I ELMy H-mode shot with attached OSP placed on the inner side of the W Ring, figure 2(a). The data were averaged over 2 ms camera integration windows, and within two closely spaced $\varnothing$1 cm spots on C and on W. ELMs were identified by the spikes in the fast
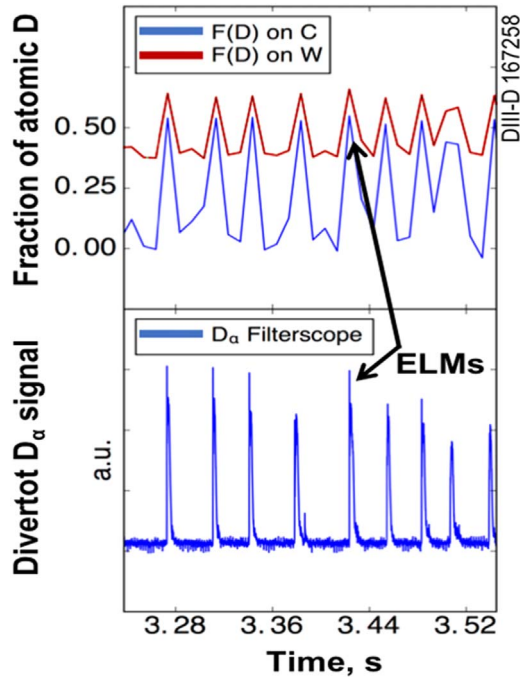
Figure 2. Fraction of atomic D (a) sourced near OSP on C and on W during a 0.3 s window of an ELMy H-mode shot during MRC, measured by fast split imaging of D_α and D_2 signal. AD divertor filterscope D_α time trace (b) is plotted to identify the ELMs.
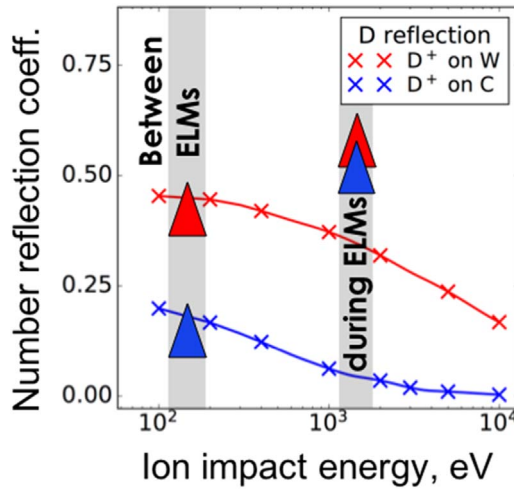

Figure 3. Calculated D number reflection coefficient, table 3 in [21] as function of D normal incidence energy (lines) and measured in MRC H-mode shot 167258, figure 2(a), fraction of D recycled in atomic form, between and during ELMs on C and on W (triangles). The vertical size of the triangles represents the experimental uncertainty.

divertor D_α signal from filterscopes, figure 2(b). F_W and F_C averaged over many ELM cycles are plotted by triangles in figure 3. For both materials the inter-ELM D reflection coefficient (triangles) are close to the values calculated for normal incidence in [21] when the D^+ incidence energy is calculated as $E_i \simeq 3T_e + 2T_i \approx 150$ eV, using the LP T_e measurements and assuming $T_e \approx T_i$. This suggests that if the recycling coefficient between ELMs is $R \approx 1$, then the atomic fraction of recycled D can be explained by reflections. The

low values for F_C are in agreement with the old H-mode data from JET-C, see Figure 7 in [10]. During ELMs the measured F increased on both W and C. This contradicts the model expectation of lower D reflection at higher E_i (assuming $E_i \approx 2$ keV ~ 4.2 times pedestal T_e during the initial ELM phase [22]). This may be indicative of the key role that other atom release processes play during ELMs, for example, ion-induced desorption and D sputtering, see figure 1 in [10] and references therein. The fraction of atoms from the surface could increase if $T_{surf.}$ increased above ~ 1100 K$^\circ$, see figure 11 in [12], but in DIII-D $T_{surf.}$ is usually much lower even during ELMs. Alternatively, the increase of the reflection coefficient can be due to more grazing ion incidence during ELMs. The measured intra-ELM reflection coefficients match the data in [23] for 2 keV D^+ at incidence angles (measured to the surface) 15° on C and 25° on W. This conjecture remains speculative because we do not have an evidence of the incidence angle change during ELMs.

In order to assess the effect of the OSP material change on the upstream D^+ density n_{D+} during the MRC, we compare the edge profiles in two similar discharges with the only difference being the OSP placement on C and on W. The changes to the equilibrium are kept minimal and only the X-point is shifted inward by ~ 5 cm, figure 4(a). n_e profiles are measured by the core and edge TS and mapped onto the normalized poloidal flux coordinate ψ_n. The density profiles of C^{6+} are measured with CER. The D^+ density is calculated as $n_D = n_e - 6 \cdot n_{C6+}$; this is accurate inside the separatrix and in the near SOL in the main chamber, where C, the main impurity ion in DIII-D, is fully ionized.

Despite the measured difference in the OSP recycling in attached H-mode shots, there was no significant difference in inter-ELM n_{D+} profiles when OSP was placed on C and on W, figure 4(b). This suggests that the fueling rate through the outer divertor was inefficient, probably due to trapping of D near the strike point. In attached L-modes, in contrast, there was a noticeable 8% increase of the edge density when OSP was placed on W, figure 4(c), qualitatively similar to the n_e density increase in L-mode seen on AUG upon transition from C to W PFCs [24]. Adding gas puff to detach the divertor in AUG removed the difference in the profiles, which supports the important role of W in the divertor for fueling in attached conditions [24] and suggests that ITER with its large detached divertor may not observe the difference either. Unlike DIII-D, AUG also observed an increase in n_e between ELMs in attached H-modes which may be due to the fact that AUG had a larger area of the divertor and the main chamber covered in W.

4. Summary

The ELM response of fuel recycling in the form of atoms and molecules has been studied in the divertor of DIII-D on biased DiMES samples and on W divertor inserts during the MRC. On DiMES an increase of the ion incidence energy E_i by 90 eV due to an electric bias of the target triggered a temporary increase of recycling by less than 10%. On all studied
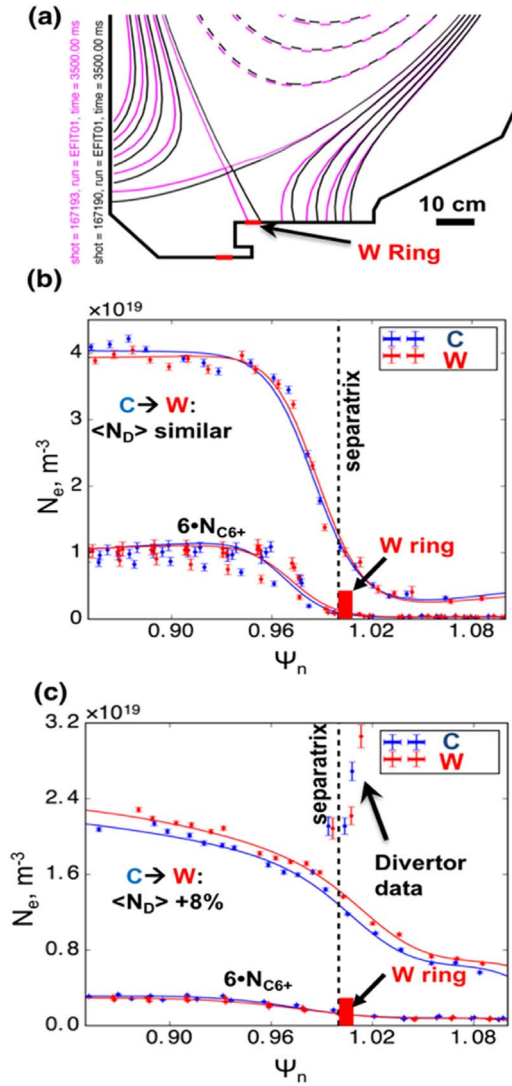
Figure 4. (a) Change of the divertor equilibrium in order to move OSP from C to the inboard side of the W Ring. In H-mode (b) there is no significant change of the edge n_e when OSP is moved from C to W, while in L-mode (c) there is an 8% increase in the edge n_e. The N_{C6+} profiles in (b), (c) show that there is no change in impurity profiles in both L- and H-modes in response to the OSP shift on W. Solid lines show polynomial fit to the data.

metals that increase was due to an extra atomic D release, whereas on C the increase was also due to ion-induced molecular D_2 re-emission. This effect is likely even stronger during ELMs, which add in excess of 1 keV to the inter-ELM ion energy. In an H-mode discharge with Type-I ELMs the inter-ELM fraction F of D recycled in the form of atoms was ~4 times higher on W than on C, consistent with expectations of the reflection model [21]. During ELMs, *F* increased despite the expectations for prompt reflections. Possible explanations argue that during ELMs D sources other than prompt reflection become important or that the incidence angle of ions becomes more grazing leading to an increase in the reflection probability.

If the atomic D population is mostly due to reflections, it can be expected that the increase of the number and the

energy of the reflected D atoms on W as compared to C will lead to more efficient divertor fueling with W in the divertor. This hypothesis was tested during the MRC, where W under the OSP has led to a moderate 8% increase of the midplane density in L-mode scenarios. This is attributed to the deeper penetration and higher flux of fast reflected D on W compared to C. Conversely, during H-modes, the midplane profiles were not affected, probably because of higher trapping of D in the divertor and lower contribution of divertor neutrals to the edge fueling.

In ITER the impact of the PFC materials on neutral fueling in the main chamber will be reduced compared to the present-day machines due to the opacity of the SOL. Divertor detachment will inhibit the prompt high-energy D^+ reflection source. The discussed material properties may become important if ELMs burn through the detached plasma and make the strike point re-attach. Then, the difference in the energy and the number of the recycled neutral atoms can influence the local plasma conditions and the following onset of detachment.

Acknowledgments

ORCID iDs

I Bykov ⓘ https://orcid.org/0000-0001-6519-6081
D L Rudakov ⓘ https://orcid.org/0000-0002-5266-4269
J Guterl ⓘ https://orcid.org/0000-0002-1049-3094
J A Boedo ⓘ https://orcid.org/0000-0003-2230-4112
C P Chrobak ⓘ https://orcid.org/0000-0002-8177-4416
T Abrams ⓘ https://orcid.org/0000-0002-9605-6871
D M Thomas ⓘ https://orcid.org/0000-0002-1217-7333

References

[1] Romanelli F *et al* 2013 *Nucl. Fusion* **53** 104002
[2] Neu R *et al* 2013 *J. Nucl. Mater.* **438** S34–41
[3] Stefanikova E *et al* 2018 *Nucl. Fusion* **58** 056010
[4] Wolfrum E *et al* 2017 *Nucl. Mater. Energy* **12** 18–27
[5] Luxon J L 2002 *Nucl. Fusion* **42** 614
[6] Bykov I *et al* 2017 *Phys. Scr.* **2017** 014034
[7] Rudakov D L *et al* 2017 *Fusion Eng. Des.* **124** 196
[8] Bykov I *et al* 2017 *Nucl. Mater. Energy* **12** 379–85
[9] Moyer R A *et al* 2018 *Rev. Sci. Instr.* **89** 10E106
[10] Pospieszczyk A *et al* 2005 *J. Nucl. Mater.* **337-339** 500–4
[11] Summers H P 2004 The ADAS User Manual, version 2.6
[12] Mertens P *et al* 2001 *Plasma Phys. Control. Fusion* **43** A349–73
[13] Scherzer B M U, Wang J and Möller W 1990 *J. Nucl. Mater.* **176&177** 208–12
[14] Couturie P *et al* 1990 *J. Nucl. Mater.* **176&177** 825–9
[15] Morita K and Hasebe Y 1990 *J. Nucl. Mater.* **176&177** 825–9
[16] Schmid K 2016 *Phys. Scr.* **2016** 014025
[17] Wiesen S *et al* 2017 *Nucl. Fusion* **57** 066024
[18] Abrams T *et al* 2018 *Nucl. Mater. Energy* **17** 164–73
[19] Hollmann E M *et al* 2006 *Plasma Phys. Control. Fusion* **48** 1165
[20] Unterberg E A *et al* 2011 *J. Nucl. Mater.* **415** S740–7
[21] Meluzova S *et al Nucl. Inst. Methods Phys. Res.* B **460** 4–9
[22] Guillemaut C *et al* 2016 *Phys. Scr.* **T167** 014005
[23] Babenko P Y *et al* 2017 *Nucl. Inst. Methods Phys. Res.* B **406** 538–42
[24] Lunt T, Reimold F, Wolfrum E, Carralero D, Feng Y, Schmid K and the ASDEX Upgrade Team 2017 *Plasma Phys. Control. Fusion* **59** 055016